J Mater Sci: Mater Med (2015) 26:37
DOI 10.1007/s10856-014-5375-1

Mechanical characterization of electrospun gelatin scaffolds cross-linked by glucose

Kaido Siimon · Hele Siimon · Martin Järvekülg

Received: 24 May 2014 / Accepted: 12 September 2014 / Published online: 13 January 2015

Abstract Nanofibrous gelatin scaffolds were prepared by electrospinning from aqueous acetic acid and cross-linked thermally by glucose. The effect of the amount of glucose used as cross-linking agent on the mechanical properties of gelatin fibres was studied in this paper. The elastic modulus of gelatin fibres cross-linked by glucose was determined by modelling the behaviour of the meshes during tensile test. The model draws connections between the elastic moduli of a fibrous mesh and the fibre material and allows evaluation of elastic modulus of the fibre material. It was found that cross-linking by glucose increases the elastic modulus of gelatin fibres from 0.3 GPa at 0 % glucose content to 1.1 GPa at 15 % glucose content. This makes fibrous gelatin scaffolds cross-linked by glucose a promising material for biomedical applications.

1 Introduction

Low mechanical strength has been limiting the use of fibrous gelatin in various applications, including biomedicine. Glucose has many advantages (biocompatibility, non-toxicity, cost-effectiveness) compared to widely used chemical cross-linking agents like dialdehydes. However, glucose alone has been reported to be a relatively ineffective cross-linking agent [1], mostly because the formation of glucose cross-links requires glucose molecules to be in their linear form [2], but normally over 99 % of glucose molecules are in the closed ring form [3]. Nevertheless, amino acids and reducing sugars react at high temperatures through the Maillard reaction pathway, but the challenge has been finding a way to preserve nanofibrous scaffold structure during thermal treatment despite the low melting point of gelatin. Preparation and mechanical characterization of nanofibrous electrospun gelatin scaffolds thermally cross-linked by glucose is described in this paper.

Interest in natural fibrous materials is continuously increasing. The fibrous structure is important in various applications including biomaterials design and many technical applications. Several methods can be used to fabricate fibrous materials, including phase separation, self-assembly, surface patterning, interfacial complexation, wet-, bio-, melt- and microfluidic spinning and electrospinning [4–6], the latter being simple, low-cost, flexible and easy to scale up. Electrospun fibrous materials can be used in various applications in the biomedical field (wound dressing, tissue engineering, drug delivery and release control), cosmetics, energy storage, filtration, protective clothing, sensors, space applications, optoelectronics, and in composite materials [7, 8].

Mechanical behaviour plays a key role in many applications. Stiffness of artificial substrate is known to influence cell growth, proliferation and differentiation [9, 10] in tissue engineering applications. Strength and durability are evident necessities in applications like filtering, protective clothing and fabrics. Although different approaches have been used to study mechanical properties of electrospun meshes, exact characterization of properties of nanofibres remains a challenge for many reasons. Random fibre orientation, mechanical anisotropy resulting from lengthwise orientation of polymer chains in electrospun fibres, the orientation of macromolecules, fibre size and humidity

K. Siimon (✉) · H. Siimon · M. Järvekülg
Institute of Physics, University of Tartu, Ravila 14c, 50411 Tartu, Estonia
e-mail: kaido.siimon@ut.ee

M. Järvekülg
Estonian Nanotechnology Competence Center, Tartu, Estonia

greatly influence fibre properties [11–13]. Furthermore, the stress–strain behaviour of electrospun fibres has been found to be different from bulk material from which it was prepared [14], making evaluation of fibre properties even harder. A variety of approaches have been applied towards mechanical characterization of nanofibres and scaffolds by employing nanoindentation, bending tests, resonance frequency measurements and tensile tests [15–17]. Mechanical properties of fibrous materials have been modelled at micro- and macro-scale in various ways mostly based on bending or tension testing, including direct calculation from experimental data, approaches based on friction, finite element analysis and analytical models [18] and using a probability density function [19].

Gelatin is a protein derived by hydrolysis from collagen, a naturally occurring protein most abundant in connective tissue. Electrospun gelatin fibres are water-soluble and must be cross-linked to make them insoluble and thus usable in practical applications. Cross-linking decreases solubility by creating chemical bonds between polymer chains. It has also been shown to increase mechanical strength (e.g. elastic modulus [20] and shear modulus [21]) of fibrous gelatin-based materials. Cross-linking of gelatin fibres can be carried out by various chemical methods [22–24], enzymatic [25] and physical [26] means or a combination of these. Gelatin can also be cross-linked thermally [27], although physical treatment generally results in a low degree of cross-linking [28] and the use of cross-linking agents can enhance the properties of the material much further. However, most chemical cross-linkers are costly, more or less toxic and even the safer ones have been found to have negative effects, for example EDC has been shown to reduce the ability of fibroblasts to proliferate [29].

The presence of sugars can alter the conformation and interactions of proteins, enable the Maillard reaction to take place and has an effect on the cross-linking process [30–32]. Thus, adding sugars to gelatin scaffolds could help us to enhance mechanical properties of the fibres by controlling the extent of cross-linking. Therefore, it is necessary to study the effect of glucose cross-linking on mechanical properties of electrospun fibres.

2 Materials and methods

2.1 Preparation of fibrous scaffolds

Gelatin type A from porcine skin, glucose and glacial acetic acid were purchased from Sigma-Aldrich. Gelatin was mixed with glucose so that various mixtures contained 0–15 % glucose. The mixtures were dissolved in 10 M aqueous acetic acid to obtain 25 % solutions. Fibrous scaffolds were prepared from these solutions by electrospinning. A syringe containing gelatin-glucose solution was mounted on a New Era Pump Systems NE-511 pump operating at 6–8 µl/min. High voltage (17.5 kV) was applied to metallic syringe needle using Heinzinger LNC 30,000 high voltage power supply. A grounded target was placed at 14 cm distance from the needle tip. Fibrous meshes were collected from the target after electrospinning and stored for further treatment.

Fibrous glucose-containing gelatin scaffolds were cross-linked by placing them in a preheated oven for 3 h. In order to avoid thermal degradation of gelatin while ensuring proper cross-linking [33] and to operate above melting point and caramelization temperature of glucose, cross-linking was carried out at 170–175 °C.

2.2 Scanning electron microscopy

The scaffolds were analysed by SEM before and after cross-linking. Samples were dried using Leica EM CPD300 critical point drier and covered with 5 nm layer of gold using Polaron SC7640 sputter coater. Fibre diameters were measured from 21,000 times magnified SEM images.

2.3 Tensile test

Electrospun scaffolds were cut into rectangular segments and their dimensions and weight were measured. Smaller, 3 × 1.5 cm samples were cut out from these scaffolds, fixed between clamps and subjected to tensile testing. Tensile test was carried out using a self-built tensile testing station (10 µm distance measurement accuracy) equipped with Sauter FH100 force sensor. The samples were pulled at 5 mm/h, elongation and force were recorded. The scaffolds were photographed during tensile test and the changes in their dimensions at given elongation were evaluated using Adobe Photoshop CS2 software.

2.4 FTIR analysis

The scaffolds were analysed by FTIR before and after thermal treatment. After drying in Leica EM CPD300 critical point drier, FTIR spectra between 400 and 4,000 cm^{-1} were recorded using Bruker Vertex 70 spectrometer equipped with an attenuated total reflection (ATR) accessory. The ATR spectra were converted to absorbance spectra after baseline correction and normalized to a constant penetration depth using OPUS software.

2.5 Modelling

2.5.1 Modelling of fibre deposition

The first step of tensile test simulation was creating a virtual fibrous scaffold. This was done by simulating fibre

deposition during electrospinning. The total length of fibres per volume in the scaffold was calculated using the dimensions, weight and fibre diameter measured beforehand. Fibres were placed randomly one by one and layer by layer to form a virtual scaffold until the calculated total fibre length was reached. Based on SEM data, the fibres were assumed to be straight and remain straight during tensile test. It was observed from SEM images taken after failure that fibres in the scaffolds tested before cross-linking were pulled straight next to the ripping point and considerable orientation of the fibres towards pulling direction was detected away from the ripping point (Fig. 1a). Scaffolds tested after cross-linking revealed very little fibre orientation right next to the ripping point. Furthermore, no increase in fibre orientation was observed by SEM when the meshes were pulled only in the elastic region of the strain and removed from the tensile testing machine before ripping (Fig. 1b). This confirms the assumption that cross-links form between individual fibres as well as between gelatin molecules in each fibre and suggests that in the elastic region where deformation is small the fibres do not slide on each other and friction does not have to be taken into account when describing tensile testing of cross-linked scaffolds.

The behaviour of the scaffolds during tensile test depends on the interactions between the fibres. Non-cross-linked fibres are relatively independent of each other, the interactions between fibre segments that are in contact are weak and all the fibres tend to change their orientation in the direction of the applied force during tensile test. Friction alone causes some resistance to fibre reorientation. In case of cross-linked fibres chemical bonds have formed not only between polymer molecules inside each fibre, but also at the interceptions of fibres. These chemical bonds connecting individual fibres make the mesh structure rigid and reorientation of a fibre caused by the applied force becomes dependent on reorientation of other fibres.

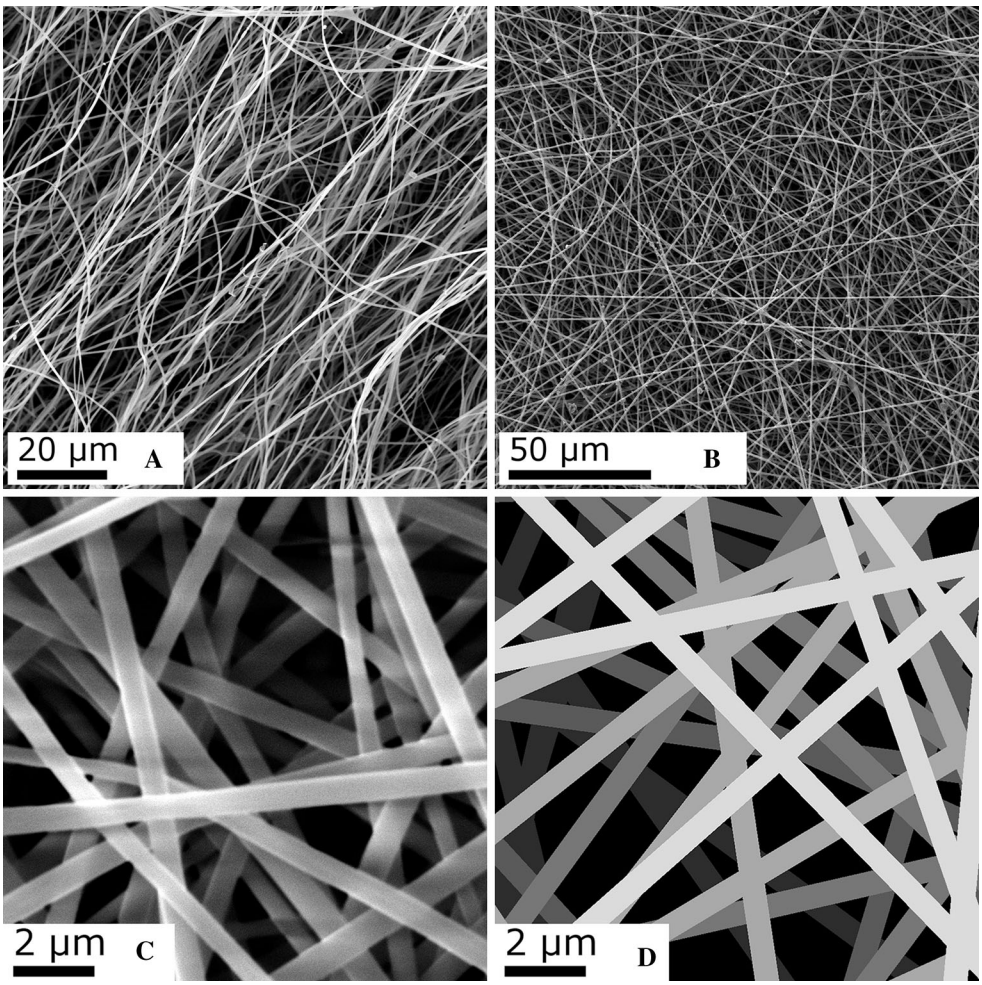

Fig. 1 **a** SEM images of non-cross-linked and **b** cross-linked gelatin scaffold after tensile testing. Images were taken at a distance of 100 µm from the ripping point. **c** 21,000 times magnified SEM image of a gelatin scaffold and **d** the virtual scaffold constructed by the model

Tensile test was simulated for cross-linked scaffolds only, because non-cross-linked scaffolds are water-soluble and thus not usable in practical applications. Comparing SEM images (Fig. 1c) with virtual meshes (Fig. 1d) constructed in the manner described above confirmed the necessary similarity between the virtual and the real scaffold.

2.5.2 Modelling of tensile test

Tensile test was simulated using virtual scaffolds constructed as described above. The goal of the simulation was to obtain the elastic region of stress–strain diagram. Fibre diameter d, elastic modulus E, a coefficient G (the value of G is proportional to shear modulus) were used as constants characterizing the material. Fibre material was considered to be brittle so that Hooke's law was valid in the whole simulated region of the stress–strain diagram. At each simulation step, a small increase was given to the length of the sample. This causes stress in the fibres. The total tensile force is equal to the sum of the forces resulting from all fibres. Decrease in mesh width (neck formation) at larger elongations is related to the strength of interactions between the fibres. It was observed experimentally that the change in shape (forming of neck due to decreased mesh width) is related to glucose concentration in the fibres. The more glucose the scaffolds contained (and therefore the higher the extent of cross-linking) the smaller was the decrease of sample width. Scaffolds containing 15 % glucose did not form any neck during tensile testing. During simulation the shape change of a piece of scaffold was determined at each step. In this work we assumed that the studied piece of scaffold remains rectangular during the test. This assumption is strictly valid for central parts of the mesh. However, if the dimensions of the scaffold piece are chosen to be small and tensile test is simulated only in the elastic region where deformation is also small, then the approximation that the scaffold is rectangular describes tensile testing accurately enough even in case of neck-formation.

Figure 2 describes the scheme of the simulation. y-axis is chosen so that it coincides with the direction of the applied force (and scaffold elongation). Each step of the simulation gives one point to the force–elongation diagram and consists of the following parts. Firstly, a small increase is given to the scaffold length, causing relative elongation of the scaffold ε_y, while the width of the scaffold is kept unchanged. This induces elongation and stress in each fibre depending on the angle α_i between the fibre and x-axis, which in return causes normal stress σ_i in ith fibre. We calculated normal stress using the equation $\sigma_i = E\varepsilon_i$, where E is the expected elastic modulus, ε_i is the relative elongation of the ith fibre and α_i is the angle between the ith fibre and x-axis. Increase in length of the scaffold causes a change $\Delta\alpha_i$ in the angle α_i. The fibres tend to be oriented towards the y-axis during tensile testing. It was taken into account that the fibres are cross-linked and relatively strong chemical bonds exist at the interceptions of individual fibres. Thus the fibres do not slide on one another and the structure is relatively rigid. Therefore torsion arises around these interceptions. Generally, the shear stress (tangential stress) τ_i in a fibre at torsion is proportional to the torsion angle. We calculated tangential stress using the equation $\tau_i = G\Delta\alpha_i$, where G is a coefficient characteristic to the fibre material and proportional to its shear modulus.

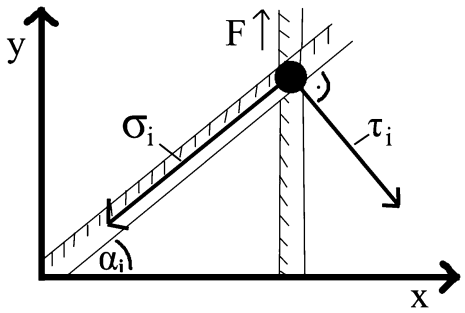

Fig. 2 The applied force causes normal stress (σ_i) and tangential stress (τ_i) in the ith fibre

Evaluation of the coefficient G is based on the following speculations. The ratio of the elastic modulus and the shear modulus depends on the Poisson coefficient, i.e., the ratio of the relative decrease of the specimen width to the relative increase of its length. The Poisson coefficient determines the change in volume of a material during tension, and the relative change of the surface area in our tensile test. Therefore we expected the E/G ratio to be connected to the relative change in the dimensions and shape of the scaffold during testing. Using the sample dimensions evaluated from the images taken during experimental tensile testing and comparing them to the dimensions calculated from the simulations at various E/G ratios, it was found that the values of E/G varied between 1.0 (for samples containing 15 % glucose) and 1.2 (for samples containing no glucose).

The second part of this simulation step takes advantage of the calculated stresses σ_i and τ_i to determine the change in mesh width. We calculated x- and y-components of normal and tangential stresses by $\sigma_{ix} = \sigma_i \cos(\alpha_i)$, $\sigma_{iy} = \sigma_i \sin(\alpha_i)$, $\tau_{ix} = \tau_i \sin(\alpha_i)$, and $\tau_{iy} = \tau_i \cos(\alpha_i)$. The y-components of σ_i and τ_i add up and their sum is balanced by the applied force. The direction of the x-components of σ_i and τ_i is determined by the angle α_i. The x-components σ_{ix} and τ_{ix} of each fibre are directed at opposite directions. The difference between their values is related to the change in fibre orientation and the decrease in scaffold width. Additionally, it gives rise to neck formation during testing.

It must be mentioned that the sum of forces resulting from the x-components of the stresses in all fibres is equal to zero, whereas the difference between σ_{ix} and τ_{ix} in each individual fibre contributes to neck formation. The sum of y-components of the stresses in all the fibres is proportional to the applied force, $F_y = (\pi d^2/4)\sum_i (\sigma_{iy} + \tau_{iy})$. The force causing the narrowing of the scaffold is caused by the differences in stress components, $F_x = (\pi d^2/4)\sum_i |\sigma_{ix} - \tau_{ix}|$. Relative decrease of the mesh width, ε_x, follows from the equation $\frac{\varepsilon_x}{\varepsilon_y} = \frac{F_x}{F_y}$, which gives

$$\varepsilon_x = \varepsilon_y . \frac{\sum_i |\sigma_i - \tau_i|}{\sum_i (\sigma_i + \tau_i)}.$$

Finally, the values of ε_y and ε_x were used to recalculate fibre lengths, stress in the fibres, and the total force F_y stretching the scaffold. The force directly causing elongation of the sample was calculated as the sum of forces determined for all fibres. In this way, tensile test was simulated by firstly calculating new dimensions of the sample, and secondly the force applied in the y-direction. So, step by step, the force-strain diagram was generated. Tensile test was simulated, adjusting the hypothetic elastic modulus, until the elastic region of experimental tensile test graph and the simulated tensile test graph overlapped. The elastic modulus of the fibre material was found for all glucose concentrations in this manner.

3 Results

3.1 Preparation of fibrous scaffolds

Fibrous gelatin scaffolds containing different amounts of glucose were prepared by electrospinning. Fibres can be produced by electrospinning gelatin from aqueous acetic acid only when the concentration of acetic acid is sufficiently high [34]. 10 M aqueous acetic acid was found to be suitable for electrospinning all the mixtures of gelatin and glucose used in this work, allowing problem-free production of fibres using a wide range of process parameters. Scaffolds were analysed by SEM. Fibres were smooth and without beads. Maximum glucose content in the fibres was kept at 15 %, because the scaffolds containing more glucose became brittle and broke easily after cross-linking. Fibre diameters were measured from 21,000 times magnified SEM images and averaged. Average fibre diameters were strongly influenced by electrospinning parameters (pumping speed, voltage, distance between needle tip and collector, relative air humidity). For example, the average fibre diameters of pure gelatin scaffolds prepared using different process parameters varied between 280 and 575 nm. Therefore, the fibre diameters of every sample used in tensile testing were measured individually. The scaffolds were cross-linked thermally by glucose at 170–175 °C. In order to ensure proper cross-linking while maintaining structural integrity of the mesh, the oven must be heated to this temperature before inserting the meshes. 170–175 °C was the chosen temperature, because at too low temperatures gelatin melts and the fibrous scaffold structure is destroyed. Additionally, operating above melting point and caramelization temperature of glucose supports the cross-linking process. As a result, 50–110 μm thick gelatin scaffolds cross-linked thermally by glucose were successfully prepared. Length of fibre per volume and porosity were calculated before tensile test. Porosity of the scaffolds varied between 78 and 87 % and seemed to be quite random. No correlation was found between scaffold porosity and composition, but scaffolds consisting of fibres with smaller diameters seemed to have higher porosity. This indicates that porosity of the material is greatly influenced by the randomness of electrospinning process.

3.2 Tensile test and simulation

Tensile tests were carried out for electrospun gelatin scaffolds cross-linked by various amounts of glucose. Force and elongation were measured during the test. A short elastic region was found to be typical (Fig. 3a). Considerable elongation was seen in the final part of the diagram as the material was slowly ripped apart. Relatively long experimentally determined plastic region was not simulated, because structural changes contribute greatly to the shape of this region and the approximation of straight fibres is not valid any more, and the aim of this study was to evaluate elastic properties of fibre material.

In order to compare the influence of E and the influence of E/G ratio on the results, tensile test was simulated using a wide range of values of E and E/G ratio. Typical results of the calculated force–elongation diagrams are shown in Fig. 3b, c. The applied force calculated from the model is proportional to the number of fibres in a particular scaffold. Therefore, the force is proportional to the total length of the fibres in each scaffold. The total force applied to the scaffold is also proportional to the cross-section area, since the force contributions of fibres are multiplications of stress and cross-section area $\pi d^2/4$, where d is the fibre diameter. The diameter and the total length of the fibres as well as the initial length and width of the mesh used in the calculations were determined experimentally beforehand. It can be seen (Fig. 3b, c) that the calculated applied force strongly depends on the elastic modulus of the fibre material whereas the dependence on the E/G ratio is rather weak.

Poisson's ratio of the fibre material was determined from the calculations presented in Fig. 4. As expected, it increases with the E/G ratio, while at E = G it is equal to

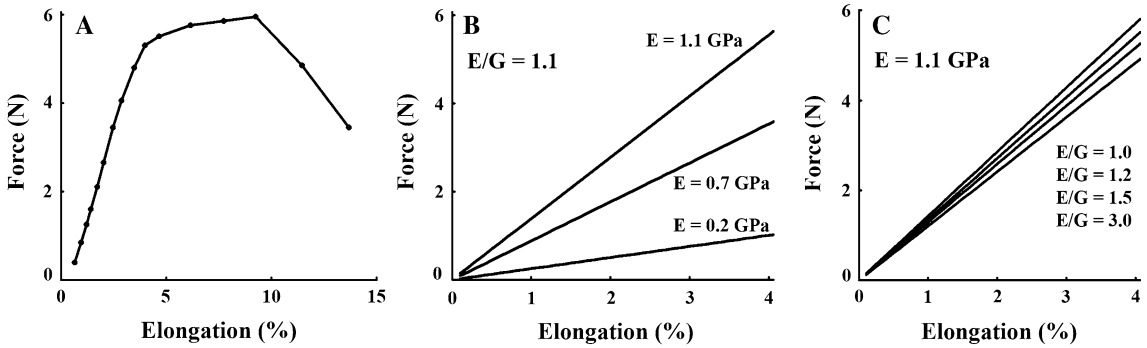

Fig. 3 Experimental tensile test (**a**) and simulation results demonstrating the effect of elastic modulus (**b**) and E/G ratio (**c**) on force–elongation curve in the elastic region

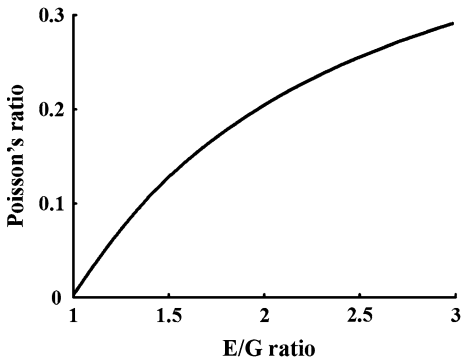

Fig. 4 Dependence between Poisson's ratio and E/G ratio

zero—no decrease of the scaffold width is observed in this case. These results are in accordance with experimental observations. Pure gelatin scaffolds showed considerable neck formation during tensile test, while the width of scaffolds containing 15 % glucose did not change at all during the test.

3.3 Elastic modulus

The elastic modulus of the fibre material was determined for samples prepared using 0–15 % glucose. It was found (Fig. 5a) that cross-linking by glucose considerably increases the elastic modulus of gelatin fibres from about 0.3 GPa (0 % glucose) to 1.1 GPa (15 % glucose). Simulation results were used to draw connections between the elastic modulus of the scaffold and the elastic modulus of the fibre material (Fig. 5b) at different *E*/*G* ratios calculated for a wider range of values of *E*. The analysis revealed that the elastic modulus of the fibre material exceeds the elastic modulus of the scaffold 8–9 times. These results seem to be reliable, taking into account the porosity and fibrous structure of the mesh.

3.4 FTIR analysis

FTIR was used to study the changes brought about by thermal treatment of the scaffolds and to confirm cross-linking. Intensity of the amide I band (peaks at 1,657, 1,640 and 1,631 cm^{-1}, mainly C=O vibrations [35]) increased and in case of glucose-containing scaffolds intensity of peaks at 1,081 and 1,035 cm^{-1} (mainly CO vibrations overlapping with other vibrations in glucose [36]) decreased considerably after thermal treatment of the scaffolds (Fig. 6). These changes were the greater the more glucose the scaffolds contained (in case of pure gelatin scaffolds the increase of the intensity of the amide I band was the only major change in spectrum). This suggests that the main reaction occurring during thermal treatment of

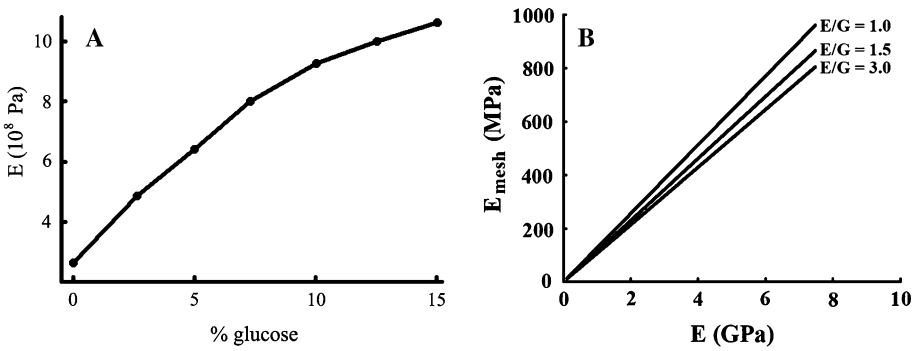

Fig. 5 **a** The effect of glucose concentration on elastic modulus of gelatin fibres; **b** Dependence between elastic modulus of the fibre material and elastic modulus of the scaffold

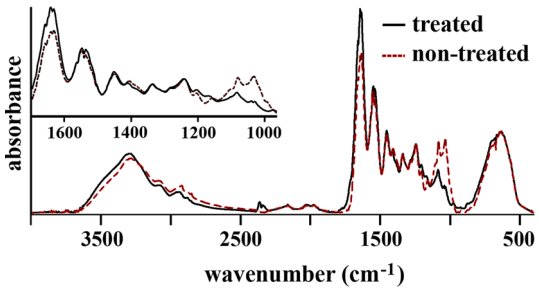

Fig. 6 FTIR spectra of the scaffolds before and after thermal treatment

glucose-containing scaffolds is indeed the Maillard reaction. Lesser changes were detected at 3,285, 3,077 cm^{-1} (OH and NH vibrations), 2,939 and 2,879 cm^{-1} (CH_2 asymmetric and symmetric vibrations respectively), 1,562, 1,547 and 1,535 cm^{-1} (the amide II band, mainly NH bending) [37].

4 Discussion

The model used in this work describes mechanical behaviour of fibrous cross-linked or otherwise interconnected materials and allows simulating tensile test in the elastic region. Remaining in the elastic region is related to the approximation that the fibres in the concerned part of a scaffold are straight during tensile test and do not slide on each other. This assumption is only valid if there are chemical bonds present at fibre interceptions. In case of gelatin scaffolds, the fibres must be cross-linked to make them insoluble and observations considered above indicate that chemical bonds appear between individual fibres during cross-linking. On a large scale, electrospun fibres are deposited in spirals, but considering the fibres to be straight is a good approximation because of the cross-links at fibre interceptions and the fact that the model operates in the elastic region. In any case, it is the elastic region that is of importance in most applications. However, for brittle fibre materials with no plastic deformation one may determine the maximum normal and tangential stresses to simulate the formation of stress–strain curve for a scaffold. Performing such simulations showed that failure of the fibres one by one leads to plastic deformation of a scaffold.

Tensile test was simulated for a small part of a scaffold and this part was assumed to remain rectangular during the simulation. Such assumption is exactly valid for all parts of the scaffold, if the width of the sample does not change during the test. Considerable neck-formation was observed in case of pure gelatin and non-cross-linked scaffolds, leading to the conclusion that forces affecting the edges of the rectangular parts of the scaffold do not remain parallel to the force applied to the sample during the test. Friction at the sample fixation point creates a force perpendicular to the applied force. Therefore, the accuracy of the model is the better the less neck-formation is observed. It remains to be clarified whether the model can also be applied to non-cross-linked scaffolds.

One of the challenges in the field of mechanical characterization of electrospun materials is achieving comparability. Cross-linking has been shown to increase elastic modulus of electrospun gelatin, but values determined by different authors vary a lot. Comparing the results is difficult not only because different techniques are used to characterize mechanical properties of nanofibres, but also because various cross-linking agents are used. For example, cross-linking gelatin by glutaraldehyde has been shown to increase the elastic modulus of electrospun gelatin mesh up to 21 MPa [38], whereas cross-linking by genipin has been shown to increase the elastic modulus of gelatin fibres up to 990 MPa [39]. Two major aspects that could cause possible errors were observed while carrying out the experimental part of this work. Firstly, porosity of the samples prepared from the same solution using the same electrospinning parameters varied up to 10 % simply because of the randomness of electrospinning process. The simulation revealed that the variations in mechanical properties caused by random fibre placement are in the same order of magnitude. Secondly, the randomness of porosity coming from casual orientation of the fibres inherent to electrospinning causes randomness of scaffold thickness. Mechanical stress is calculated by dividing force by cross-section area. Therefore, the non-uniform thickness of the scaffold causes errors in determining the cross-section area of the sample, which in return causes errors in determining the stress. These errors can be somewhat lessened by calculating the total length of the fibres per volume. In this case, the applied force can be presented as the function of the cross-section area of the fibres, and the fibre diameters can be measured quite accurately by SEM.

FTIR analysis confirmed the assumption that the major reaction occurring during thermal treatment is the Maillard reaction. Gelatin and glucose in the scaffolds react with each other, but this alone does not prove the formation of cross-links between gelatin molecules. However, if cross-links wouldn't have formed, then it would be hard to explain the increase in elastic modulus of the material. Therefore FTIR analysis coupled with tensile test and modelling results suggests that the presence of glucose increases the extent of cross-linking of gelatin scaffolds during thermal treatment.

Compared to other previously used cross-linking agents, glucose is not only biocompatible and non-toxic, but also relatively cheap. The whole process of producing cross-linked and thus insoluble and durable fibrous scaffolds

described in this work uses only natural substances and easy, cost-effective methods.

5 Conclusions

Nanofibrous gelatin scaffolds containing up to 15 % glucose were prepared by electrospinning from aqueous acetic acid. At higher glucose concentrations the scaffolds become unpractically brittle after thermal treatment. The scaffolds were thermally cross-linked by glucose, which proved to be an effective cross-linking agent. Mechanical properties of the material were evaluated by tensile test and modelling. The model simulates deposition of fibres during electrospinning and tensile test of fibrous meshes in order to evaluate the elastic modulus of electrospun materials and is effective when applied to cross-linked scaffolds with bonds between both polymer molecules and at fibre interceptions. Adjusting glucose content in gelatin fibres gives us control over the elastic modulus of the fibre material in a wide range. Cross-linking by glucose increases the elastic modulus of gelatin nanofibres from 0.3 GPa at 0 % glucose content to 1.1 GPa at 15 % glucose content.

Acknowledgments This study was financially supported by the European Union through the European Regional Development Fund via projects "Carbon Nanotube Reinforced Electrospun Nano-fibres and Yarns" (3.2.1101.12-0018), "SmaCell" (3.2.1101.12-0017) and Centre of Excellence "Mesosystems: Theory and Applications" (3.2.0101.11-0029) and Estonian Science Foundation Grant IUT2-25.

References

1. Ohan MP, Weadock KS, Dunn MG. Synergistic effects of glucose and ultraviolet irradiation on the physical properties of collagen. J Biomed Mater Res. 2002;60(3):384–91.
2. Bunn HF, Higgins PJ. Reaction of monosaccharides with proteins: possible evolutionary significance. Science. 1981; 213(4504):222–4.
3. Angyal SJ. The composition of reducing sugars in solution. Adv Carbohydr Chem Biochem. 1984;42:15–68.
4. Wang X, Ding B, Li B. Biomimetic electrospun nanofibrous structures for tissue engineering. Mater Today. 2013;16(6): 229–41.
5. Pham QP, Sharma U, Mikos AG. Electrospinning of polymeric nanofibers for tissue engineering applications: a review. Tissue Eng. 2006;12(5):1197–211.
6. Tamayol A, Akbari M, Annabi N, Paul A, Khademhosseini A, Juncker D. Fiber-based tissue engineering: progress, challenges, and opportunities. Biotechnol Adv. 2013;31:669–87.
7. Raghavan P, Lim D-H, Ahn J-H, Nah C, Sherrington DC, Ryu H-S, Ahn H-J. Electrospun polymer nanofibers: the booming cutting edge technology. React Funct Polym. 2012;72:915–30.
8. Huang Z-M, Zhang Y-Z, Kotaki M, Ramakrishna S. A review on polymer nanofibers by electrospinning and their applications in nanocomposites. Compos Sci Technol. 2003;63:2223–53.
9. Engler AJ, Sen S, Sweeney HL, Discher DE. Matrix elasticity directs stem cell lineage specification. Cell. 2006;126:677–89.
10. Rao N, Grover GN, Vincent LG, Evans SC, Choi YS, Spencer KH, Hui EE, Englerac AJ, Christman KL. A co-culture device with a tunable stiffness to understand combinatorial cell–cell and cell–matrix interactions. Integr Biol. 2013;5(11):1344–54.
11. Baji A, Mai Y-W, Wong S-C, Abtahi M, Chen P. Electrospinning of polymer nanofibers: effects on oriented morphology, structures and tensile properties. Compos Sci Technol. 2010;70:703–18.
12. Tan EPS, Ng SY, Lim CT. Tensile testing of a single ultrafine polymeric fiber. Biomaterials. 2005;26:1453–6.
13. McManus MC, Boland ED, Koo HP, Barnes CP, Pawlowski KJ, Wnek GE, Simpson DG, Bowlin GL. Mechanical properties of electrospun fibrinogen structures. Acta Biomater. 2006;2:19–28.
14. Pedicini A, Farris RJ. Mechanical behavior of electrospun polyurethane. Polymer. 2003;44:6857–62.
15. Strange DGT, Tonsomboon K, Oyen ML. Mechanical behaviour of electrospun fibre-reinforced hydrogels. J Mater Sci Mater Med. 2014;25(3):681–90.
16. Bhardwaj N, Kundu SC. Electrospinning: a fascinating fiber fabrication technique. Biotechnol Adv. 2010;28:325–47.
17. Tan EPS, Lim CT. Mechanical characterization of nanofibers—a review. Compos Sci Technol. 2006;66:1102–11.
18. Syerko E, Comas-Cardona S, Binetruy C. Models of mechanical properties/behavior of dry fibrous materials at various scales in bending and tension: a review. Compos A. 2012;43:1365–88.
19. Rizvi MS, Kumar P, Katti DS, Pal A. Mathematical model of mechanical behaviour of micro/nanofibrous materials designed for extracellular matrix substitutes. Acta Biomater. 2012;8:4111–22.
20. Zhang YZ, Venugopal J, Huang Z-M, Lim CT, Ramakrishna S. Crosslinking of the electrospun gelatin nanofibers. Polymer. 2006;47:2911–7.
21. Yang L, Fitié CFC, van der Werf KO, Bennink ML, Dijkstra PJ, Feijen J. Mechanical properties of single electrospun collagen type I fibers. Biomaterials. 2008;29:955–62.
22. Yang L-J, Ou Y-C. The micro patterning of glutaraldehyde (GA)-crosslinked gelatin and its application to cell-culture. Lab Chip. 2005;5(9):979–84.
23. Lien S-M, Ko L-Y, Huang T-J. Effect of crosslinking temperature on compression strength of gelatin scaffolds for articular cartilage tissue engineering. Mater Sci Eng C. 2010;30:631–5.
24. Zhang X, Do MD, Casey P, Sulistio A, Qiao GG, Lundin L, Lillford P, Kosaraju S. Chemical cross-linking gelatin with natural phenolic compounds as studied by high-resolution NMR spectroscopy. Biomacromolecules. 2010;11(4):1125–32.
25. Bertoni F, Barbani N, Giusti P, Ciardelli G. Transglutaminase reactivity with gelatine: perspective applications in tissue engineering. Biotechnol Lett. 2006;28(10):697–702.
26. Gorgieva S, Kokol V. Collagen- vs. gelatin-based biomaterials and their biocompatibility: review and perspectives. In: Pignatello R, editors. Biomaterials applications for nanomedicine. Rijeka, Croatia: InTech; 2011. p. 17–52.
27. Birshtein VY, Tul'chinskii VM. A study of gelatin by IR spectroscopy. Chem Nat Compd. 1982;18(6):697–700.
28. Zhan J, Lan P. The review on electrospun gelatin fiber scaffold. J Res Updates Polym Sci. 2012;1:59–71.
29. Boekema BKHL, Vlig M, Damink LO, Middelkoop E, Eummelen L, Bühren AV, Ulrich MMW. Effect of pore size and crosslinking of a novel collagen-elastin dermal substitute on wound healing. J Mater Sci Mater Med. 2014;25(2):423–33.
30. Gu X, Campbell LJ, Euston SR. Influence of sugars on the characteristics of glucono-δ-lactone-induced soy protein isolate gels. Food Hydrocoll. 2009;23:314–26.
31. Rich LM, Foegeding EA. Effects of sugars on whey protein isolate gelation. J Agric Food Chem. 2000;48(10):5046–52.
32. Cortesi R, Nastruzzi C, Davis SS. Sugar cross-linked gelatin for controlled release: microspheres and disks. Biomaterials. 1998;19(18):1641–9.

33. Kozlov PV, Burdygina GI. The structure and properties of solid gelatin and the principles of their modification. Polymer. 1983;24(6):651–66.
34. Song J-H, Kim H-E, Kim H-W. Production of electrospun gelatin nanofiber by water-based co-solvent approach. J Mater Sci Mater Med. 2008;19(1):95–102.
35. Nguyen T-H, Lee B-T. Fabrication and characterization of cross-linked gelatin electro-spun nano-fibers. J Biomed Sci Eng. 2010; 3:1117–24.
36. Ibrahim M, Alaam M, El-Haes H, Jalbout AF, de Leon A. Analysis of the structure and vibrational spectra of glucose and fructose. Eclet Quim. 2006;31(3):15–21.
37. Lin L-H, Chen K-M, Liu H-J, Chu H-C, Kuo T-C, Hwang M-C, Wang C-F. Preparation and surface activities of modified gelatin-glucose conjugates. Colloids Surf A: Physicochem Eng Asp. 2012;408:97–103.
38. Zha Z, Teng W, Markle V, Dai Z, Wu X. Fabrication of gelatin nanofibrous scaffolds using ethanol/phosphate buffer saline as a benign solvent. Biopolymers. 2012;97(12):1026–36.
39. Panzavolta S, Gioffre M, Focarete ML, Gualandi C, Foroni L. Electrospun gelatin nanofibers: optimization of genipin cross-linking to preserve fiber morphology after exposure to water. Acta Biomater. 2011;7:1702–9.